Eur. Phys. J. A **16**, 199–207 (2003)
DOI 10.1140/epja/i2002-10091-y

THE EUROPEAN PHYSICAL JOURNAL A

Search for dynamical effects in the fission decay in the 240 MeV $^{32}S + ^{100}Mo$ reaction

G. La Rana[1], A. Brondi[1], R. Moro[1,a], E. Vardaci[1], A. Ordine[1], A. Boiano[1], M.A. Di Meo[1], A. Scherillo[1], D. Fabris[2], M. Lunardon[2], G. Nebbia[2], G. Viesti[2], M. Cinausero[3], E. Fioretto[3], G. Prete[3], N. Gelli[4], and F. Lucarelli[4]

[1] Dipartimento di Scienze Fisiche, Università di Napoli "Federico II" and Istituto Nazionale di Fisica Nucleare, Via Cinthia, 80126 Napoli, Italy
[2] Dipartimento di Fisica and Istituto Nazionale di Fisica Nucleare, Padova, Italy
[3] Laboratori Nazionali di Legnaro dell' Istituto Nazionale di Fisica Nucleare, Legnaro (Padova), Italy
[4] Dipartimento di Fisica and Istituto Nazionale di Fisica Nucleare, Firenze, Italy

Received: 6 August 2002 /
Published online: 4 February 2003 –
Communicated by C. Signorini

Abstract. Light particles in coincidence with evaporation residues and heavy fragments have been measured by a 4π charged-particle detector at the INFN Laboratori Nazionali di Legnaro (Padua) for the 240 MeV $^{32}S + ^{100}Mo$ reaction leading to the ^{132}Ce composite system at 152 MeV of excitation energy. Energy spectra of the alpha-particles in coincidence with fission fragments were extracted for many correlation angles both in plane and out of plane. A prominent out-of-plane emission was observed, consistent with the pattern for the near-scission emission. From the fit to the spectra, the pre-scission alpha-particle multiplicity of 0.040 ± 0.006 was obtained. This value is reproduced by the code PACE2 without the inclusion of a delay time for fission. The presence of fast fission, which could be responsible for this result, is discussed.

PACS. 25.70.Jj Fusion and fusion-fission reactions

1 Introduction

The study of the nature and magnitude of nuclear dissipation and its effects on the fission process occurring in reactions between heavy ions at low energies (≤ 10 AMeV) has been the subject of a large variety of experimental and theoretical works [1–15]. Since the time scale of fission is thought to be affected by nuclear dissipation [16], the main goal of these studies is the use of γ-rays and light-particle emissions as probes for the dynamical evolution of the composite nuclear system in its journey from the equilibrium to the scission point. The common experimental procedure is to measure energy spectra and angular distributions of a probe of a given type in coincidence with fission fragments from which multiplicities are extracted.

The presence of dynamical effects in the fission decay is inferred on the basis of the standard statistical model [2]. There exists an energy domain [1–15] above which multiplicities of neutrons, protons, alpha-particles and GDR γ-rays yields associated to the pre-scission are under-predicted by the statistical model, and the extent of the gap usually grows with increasing excitation energy. Along with this result, it is also found that the fission fragments are usually very cold and that the emissions of GDR γ-rays and alpha-particles show signatures of a deformed emitting source.

The overall picture, suggested at first in studies involving only neutron emission [2], is that because of the nuclear viscosity the collective flow of mass from equilibrium to scission is slowed down. As an immediate consequence, particles and γ-ray emission can occur more favourably because fission cannot compete effectively in the early stages of the decay. On a time scale ground, particle/γ-ray emissions proceed with a time scale much shorter than fission time scale, differently from what is supposed in the statistical model and found at lower energies.

Several interesting modifications of the statistical model have been proposed in the literature to take explicitly into account time scales as well as viscosity [4,5,9,12, 17,18]. Following the initial idea of the "neutron clock", the common trend is to split the path from equilibrium to the scission point into two regions, the pre- and the post-saddle. The total fission time is defined as $\tau_f = \tau_d + \tau_{ssc}$, where τ_d is the pre-saddle delay, namely the characteristic time necessary for the build up of the collective motion toward the saddle point, and τ_{ssc} is the time of the path from saddle to scission. The relevant observables are

[a] e-mail: moro@na.infn.it

computed using $\tau_{\rm d}$ and $\tau_{\rm ssc}$ as free parameters, along with the other input parameters relative to the specific ingredients of the model (*i.e.*, level density, shell corrections, fission barriers...), and fitted to the experimental data.

In spite of the extensive theoretical effort, estimates of the fission time scales are quite controversial, not easily comparable on a common physical ground, and weakened by the fact that different sets of input parameters can result in equally good fits within the same model. Other important open questions remain the delicate and blurred separation between pre- and post-saddle emissions, the change in the strength of the viscosity in the pre- and post-saddle motion, and its dependence on the temperature and deformation [12,13].

The failure of the standard statistical model approach to the study of the fission decay has also triggered an enormous activity toward dynamical models [19]. Although these models are basically expected to be more realistic, much work still need to be done to reach a more comprehensive picture of the dynamical effects.

Most of the data gathered so far have been involving compound nuclei with $A \approx 200$–250. In this paper we propose to extend the study of fission dynamics to systems of intermediate fissility ($\chi = 0.5$–0.6) which carry several advantages. These systems are characterized by an evaporation residue cross-section comparable or larger than the fission cross-section, and by a shorter path in the deformation space from the saddle to scission point [20]. Consequently, in a theoretical framework in which time scale estimates rely on the model calulations, the input parameters can be further constraint through additional observables in the evaporation residue channel, and the role of the pre-saddle dynamics relative to the saddle-to-scission one is enhanced, so reducing some of the ambiguities on the not well-identified separation and interplay between pre- and post-saddle regions. Furthermore, light charged particles are expected to be emitted with much higher multiplicity in the pre-scission region and, especially alpha-particles are sensitive to the emitter deformation as well as to the yrast line at high angular momentum. Therefore, clues on the system deformation can be conveniently cumulated with the ones extracted by γ-rays studies.

Recently, the charged-particle emission in both evaporation residue and pre-scission channels has been used to get the fission delay [21] for the systems 180 MeV $^{32}\mathrm{S} + ^{109}\mathrm{Ag}$ [14], 905 MeV $^{121}\mathrm{Sb} + ^{27}\mathrm{Al}$ [6] and 247, 337 MeV $^{40}\mathrm{Ar} + ^{\rm nat}\mathrm{Ag}$ [1]. A fission delay $\tau_{\rm d}$ has been introduced in the statistical code PACE2, to fit the pre-scission multiplicity. A wide interval of time delays was obtained with values in the range 4–27×10^{-21} s.

On these grounds, we have started a research program aimed at studying the fission dynamics in systems of intermediate fissility. In this paper, we describe results of the measurement performed on the system 240 MeV $^{32}\mathrm{S} + ^{100}\mathrm{Mo}$ leading to the composite system ^{132}Ce at the excitation energy of 152 MeV. We took full advantage of the performances of the 8πLP apparatus under operation at Laboratori Nazionali di Legnaro. Energy spectra of light charged particles, in coincidence with evaporation residues and fission fragments, were measured with low energy thresholds and with an almost 4π geometry.

2 Experimental setup

The experiment was performed at the XTU Tandem-ALPI Superconducting LINAC accelerator complex of the Laboratori Nazionali di Legnaro. A 240 MeV pulsed beam of ^{32}S of about 1 pnA intensity was used to bombard a self-supporting ^{100}Mo target, 300 μg/cm^2 thick. A beam burst with frequency of about 1.25 MHz and duration of about 2 ns was used.

We used the 8πLP apparatus [22], which is a light charged-particle detector assembly which fulfils the following requirements:

a) angular coverage close to 4π,
b) compact and flexible arrangement to accommodate different trigger detectors,
c) low identification energy thresholds,
d) high granularity,
e) measurement of energy of light charged particles from heavy-ion reactions up to $\sim$ 10 AMeV of incident energy.

It consists of two detector subsystems: the WALL and the BALL. The WALL made of 116 telescopes is placed at 60 cm from the target covering an angular range from 2° to 24°. The BALL of 30 cm in diameter consists of 7 rings placed coaxially around the beam axis, each with 18 telescopes for a total number of 126 telescopes covering an angular range from 34° to 165°. The rings are labelled from A to G going from backward to forward angles each covering an angular opening of about 17°.

Particle identification is carried out by the ΔE-E method and, for particles stopping in the first stage of the telescope, by the TOF method for the particle detected in the WALL, and by the Pulse Shape Discrimination (PSD) technique for the particle detected in the BALL. The BALL silicon detectors are mounted with the rear side facing the target, in the so-called *flipped* configuration.

In this configuration we are able to measure energies up to 64 AMeV in the WALL and 34 AMeV in the BALL with energy thresholds of 0.5 MeV for protons and 2 MeV for alpha-particles.

To detect evaporation residues, the WALL detectors between 2.5° and 7.5° around the beam axis were replaced by 4 Parallel Plate Avalanche Counter modules, each one subtending a solid angle of about 0.3 msr. Each module consists of two coaxial PPACs mounted and operating in the same gas volume at a distance of 15 cm from each other. By adjusting the gas pressure, it is possible to stop the ER between the two PPACs, and let the fission fragments and elastic scattered ions to impinge on the second PPAC. Consequently, evaporation residue (ER) signals were sorted out by the first PPAC using the signal from the second PPAC as a veto.

Heavy fragments were detected in the telescopes of the ring F and G of the BALL. The PSD technique allowed

the separation between heavy fragments and light particles stopping in the same detector. Selection between symmetric and asymmetric mass splitting has been achieved in this reaction on a kinematics ground as explained later.

The acquisition system is based on a newly designed readout FAIR bus [23] and is capable of handling about 1000 input signals between energy and time. The on-line analysis of all the default 1D histograms and of about 800 2D matrices is handled by commercial VME CPUs. The whole acquisition system is accessible via Ethernet since is designed on a client/server architecture.

Data were collected requiring the OR mode between the following conditions: a) coincidence between PPAC and any particle detector to select events corresponding to light particles emitted in the evaporation residue channel, b) two-fold event in the F and G ring detectors to select events with two fission fragments, and c) coincidence between one detector of the F or G ring and all other particle detectors. During the data taking the acquisition rate was about 1.5 k events per second with dead time of $\sim 15\%$ mainly due to the conversion time and the storage of events on tape. The replay of data tape, the data sorting and analysis has been handled by the software package VISM [24].

3 Data analysis and results

The main goal of the data analysis presented is the extraction of the pre-scission multiplicity of the alpha-particles from which we estimate the fission time scale. Data on protons and alpha-particles in the ER channel have been also obtained in order to further constraint the statistical model parameters. Results reported in this paper refer to the data collected by the BALL section of the 8πLP apparatus.

3.1 Selection of the fission fragments

In order to select fission fragments out of the possible binary reaction products, we have analysed fragment-fragment coincidences. In fig. 1a and b, we show the fragment-fragment energy correlation with correlation angles in the range 68°–104° and 87°–123° corresponding to two fragments detected by two different telescopes in the same ring G and in the rings F-G, respectively. The data have been summed over all the combinations of detectors belonging to the ring F and G . In fig. 1a the energy distribution is compatible with the presence of Deep Inelastic Collisions (DIC) which produces target-like and projectile-like fragments. A simulation of the DIC, performed by the code GANES, gives for the folding-angle distribution a bell shape centered around 88°, ranging from 75° to 100°. As regards the fission process, the code predicts a bell-shaped distribution centered around 100°, ranging from 90° to 110°. Taking the events of fig. 1b, which correspond to an angular range centered around the most probable folding angle for fission, one can be confident that most of the events are associated with fission fragments. This

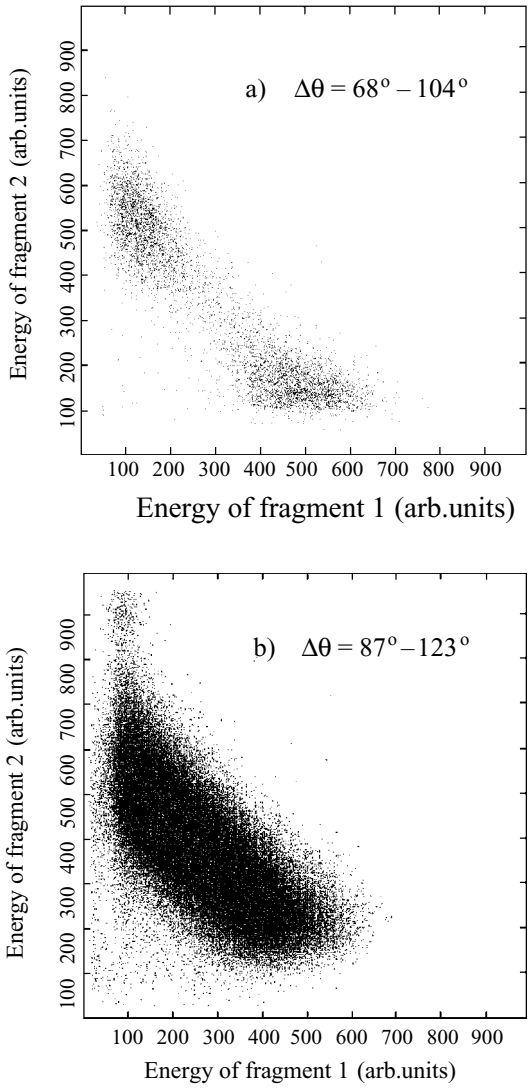

Fig. 1. Energy correlation between fragments in two different windows of the correlation angle.

conclusion is supported by the fact that the multiplicity of pre- and post-scission alpha-particles, extracted by the procedure described in the following, do not change significantly when the event selection is restricted to regions with nearly the same energy for the two fragments.

3.2 Alpha-particle emission in the fission channel

Laboratory energy spectra of the alpha-particles in triple coincidence (fragment-fragment-particle) were extracted for all the correlation angles allowed by the geometry (12 in plane and 56 out of plane). Some of the multiplicity spectra are shown as histograms in figs. 2, 3, 4 and 5.

Figure 2 refers to the 12 in-plane angle correlations, while figs. 3, 4 and 5 refer to the out-of-plane multiplicity distributions.

Each alpha-particle spectrum has been obtained as the sum of alpha-particle spectra corresponding to the same

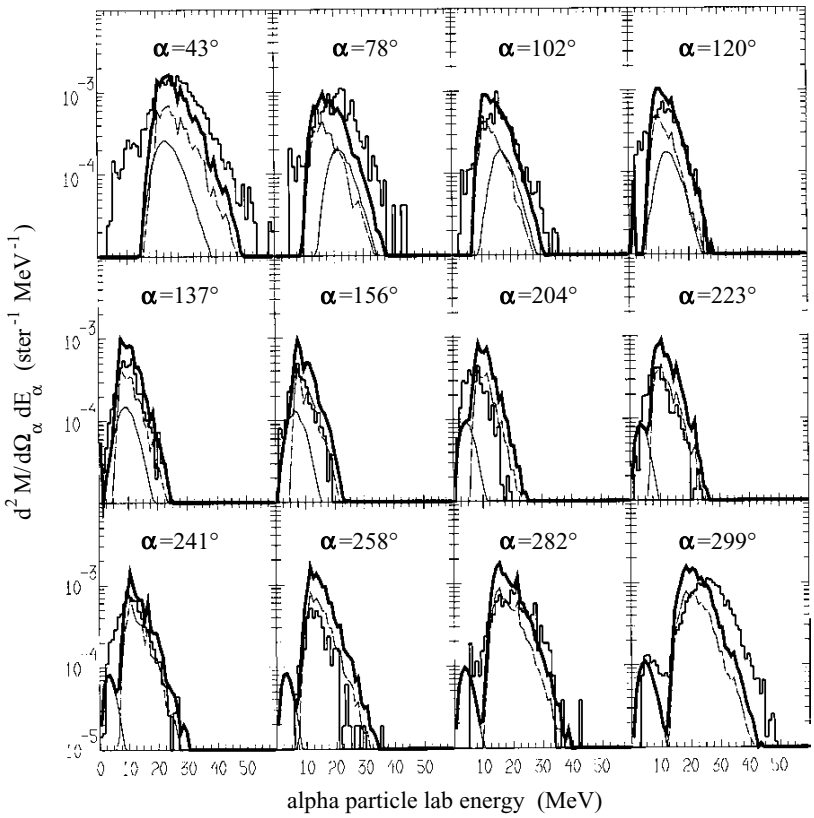

Fig. 2. In-plane ($\beta = 0$) multiplicity spectra of alpha-particles in the fission channel.

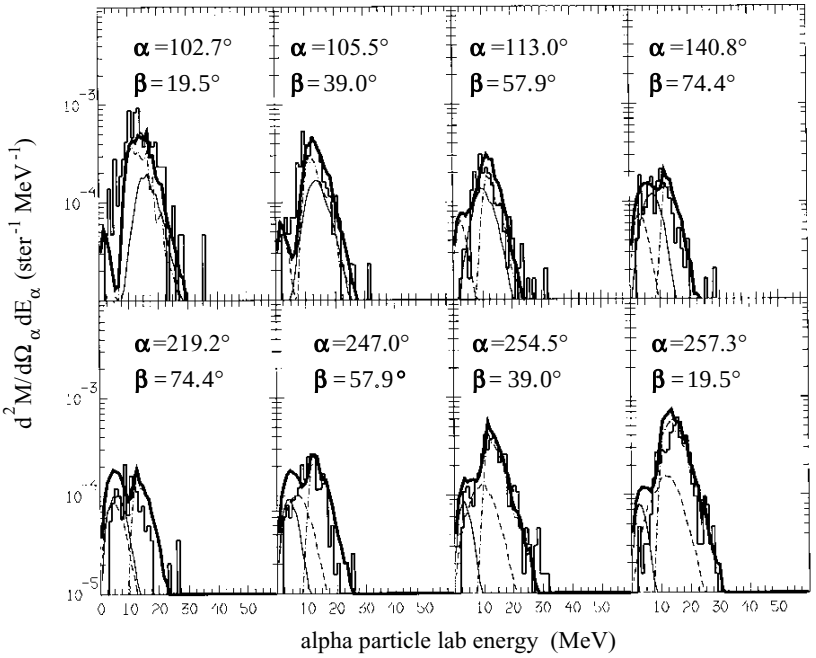

Fig. 3. Out-of-plane multiplicity spectra of alpha-particles in the fission channel (ring D).

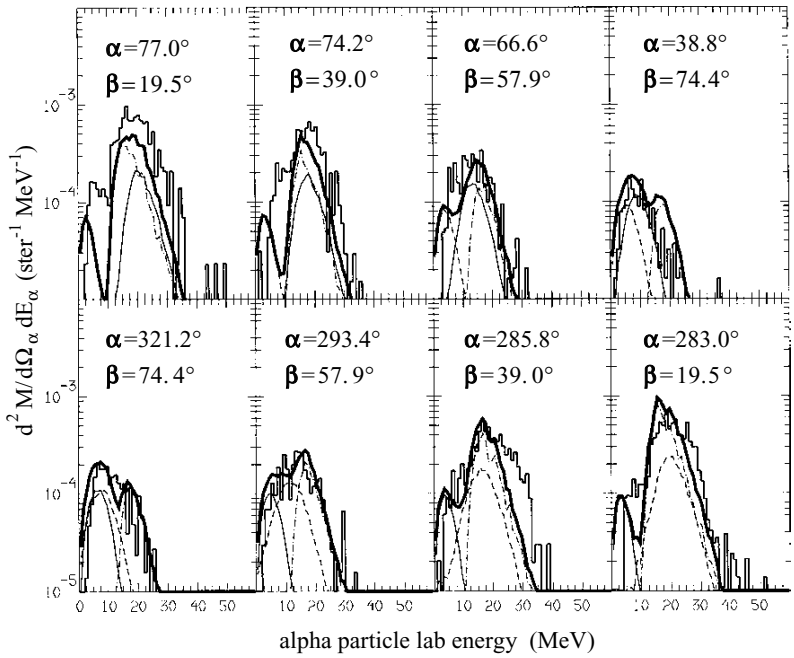

Fig. 4. Out-of-plane multiplicity spectra of alpha-particles in the fission channel (ring E).

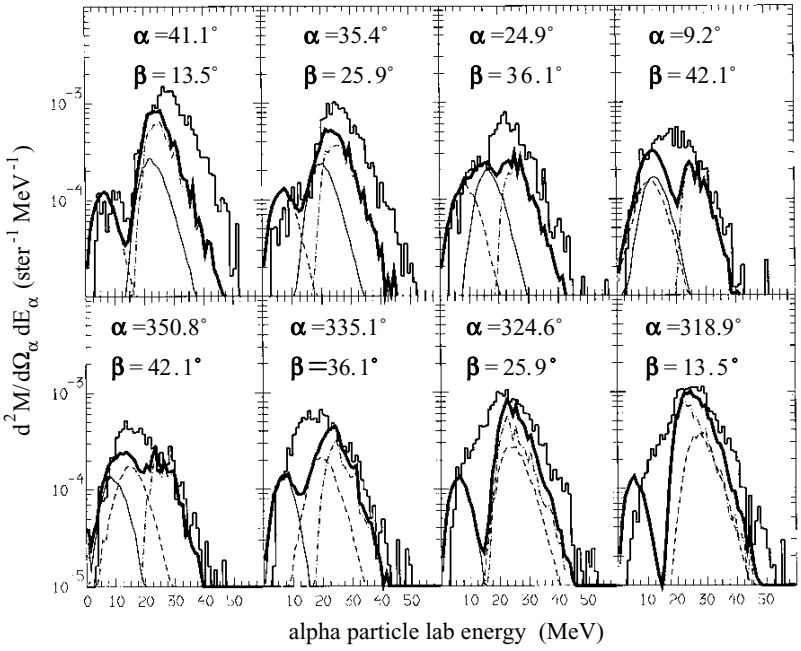

Fig. 5. Out-of-plane multiplicity spectra of alpha-particles in the fission channel (ring G).

in-plane and out-of-plane angles, and normalized to the number of its corresponding trigger fragment-fragment events.

The particle detector position has been identified with respect to a trigger plane, defined by the position of the two fired fragment detectors, using in-plane (α) and out-of-plane (β) angles. The values of these, ranging from 0° to 360° and from 0° to 90°, respectively, are shown in figs. 2, 3, 4 and 5. Rings D and E cover the same out-of-plane angular range, which is the largest with respect to the other rings, and ring G is positioned at most forward in-plane angles.

In order to extract the pre- and post-scission integrated multiplicities, alpha-particle spectra have been analysed considering three evaporative sources: the composite nucleus prior to scission (CE) and the two fully accelerated fission fragments (F1 and F2). We have used a well-established procedure which employs the Monte Carlo Statistical code GANES [25,26,6,1]. Alpha-particle evaporative spectra are computed separately for each

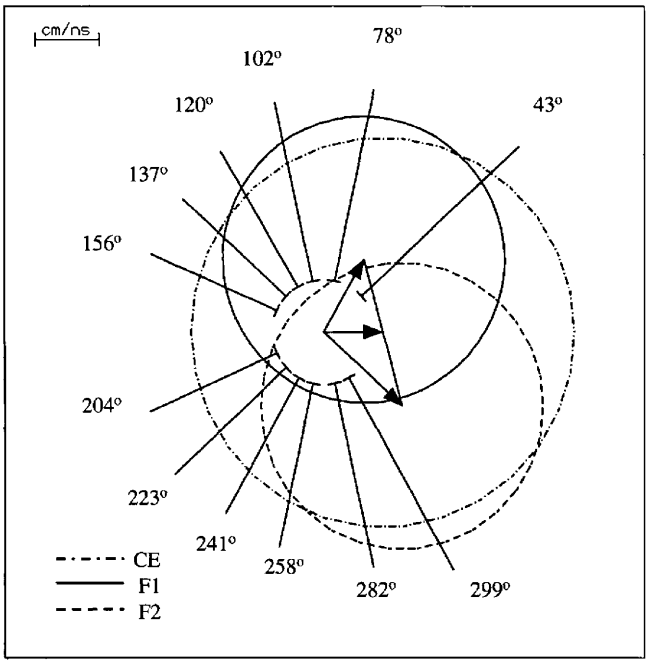

Fig. 6. In-plane velocity vector diagram for the reaction 240 MeV $^{32}S + ^{100}Mo$.

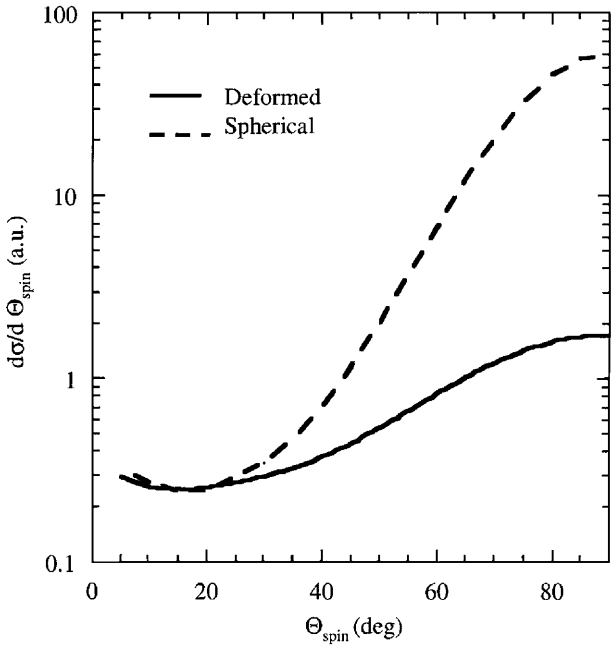

Fig. 7. Center-of-mass alpha-particle angular distributions calculated by the code GANES for the emission from a compound nucleus with $J = 85\hbar$, in the spherical and deformed ($b/a = 3$) case. $\Theta_{\rm spin}$ is the angle with respect to the spin.

source of emission in the trigger configuration defined in the experiment, taking into account the detection geometry. Afterwords, the calculated spectra are normalised to the experimental ones, and the integrated multiplicities are calculated for each emitting source. Since the components overlap in the experimental data, the normalization procedure starts by establishing upper limits for the contribution of each component from the region of the spectra where one component is prominent with respect to the other ones.

An important guide for this procedure is the velocity vector diagram as shown in fig. 6 for the in-plane measurements. In the figure the arrows indicate the compound-nucleus velocity and the fragment velocities detected in the F-G rings. The radius of each of the three circles, which are centred at the tip of the vector velocities, represents the average velocity of the alpha-particles in the emitter reference frame, namely the composite system (dot-dashed line) and the fission fragments (solid and dashed lines). The position of the detectors are superimposed on the diagram and the energy thresholds are indicated by short bars normal to the angle lines. An upper limit for the CE was assigned in the normalization procedure by reference to the spectra at in-plane correlation angles of 204°, 223° and 241°. Similarly, an upper limit for the F1 and F2 emission was set by the spectra at 78 ° and 299°, respectively. The curves superimposed on the histograms in figs. 2, 3, 4 and 5 represent calculated multiplicity spectra for CE (dot-dashed curves), F1 (light solid line) and F2 (dashed line) components, along with their sum (dark solid line).

The code GANES simulates the single-step particle emission from deformed nuclei whose shape is parametrized in terms of Cassini ovals and the evaporation barriers are determined by the extent of the deformation. The single-step approximation can be considered reasonable in the case of alpha-particle pre-scission emission characterized by low multiplicity and high first-chance emission probability. In our calculation, deformation is introduced only for the CE emission, whereas fragment evaporation is assumed from spherical nuclei. GANES simulations were made with two free parameters: the deformation parameter $0 < \epsilon < 1$, and the fractional energy loss (FEL) prior to charged-particle evaporation. The compound-nucleus angular momentum has been fixed to the average value of $85\hbar$ predicted by the multistep Monte Carlo code PACE2 which takes into account the competition between fission and evaporation channels. The deformation of the emitter affects both the mean energy of the evaporated charged particle, because of the change in the evaporation barriers, and the out-of-plane angular distribution, because of the increase in the moment of inertia. In our data the best fit of the energy spectra provides for the CE component $\epsilon = 0.8$ ($b/a = 3$) and FEL = 0.15. This emitter deformation results into mean energies of the alpha-particles which are ≈ 2 MeV lower than those expected in the case of a spherical emitter.

It is important to stress that to reproduce both the energy spectra and the out-of-plane angular distributions imposes very strong constraints on the model parameters. In this respect, the alpha-particle angular distribution is very sensitive to the nuclear deformation, setting a lower limit for $\epsilon = 0.7$.

The effects of the deformation can be very effectively seen in the center-of-mass angular distribution with respect to the spin. In fig. 7 we show, as dashed line, the angular distribution calculated with respect to the spin

of the alpha-particles emitted from the spherical nucleus. The same angular distribution but calculated for the deformed nucleus is shown as solid line. The anisotropy for the spherical emitter is about 30 times larger than that expected for the deformed emitter because of the different moment of inertia.

Assuming the evaporation from the three emitting sources, the bulk of the experimental spectra is very well reproduced, also considering the wide angular coverage of the detecting array. Nevertheless, a detailed inspection reveals contributions not accounted for by the CE and FE which are mainly of two kinds: an excess of high-energy alpha-particles at most forward angles, and a surplus of particles with energies intermediate between those corresponding to CE and FE. These two types of contributions have already been observed in other experiments of the same kind as presented here [1,6,14] and have been ascribed to pre-equilibrium and near-scission emission [27–29], respectively.

The in-plane angular distribution in fig. 2 and the out-of-plane one in ring G (fig. 5) are most suited to clarify the pattern of the excess at higher energies. In fig. 2, this excess disappears when going from forward to backward angles; in fig. 5, the top and bottom rows show clearly the gradual disappearance of the higher-energy component when the detection position moves to larger out-of-plane angles. The angular pattern observed in plane, and, more noticeably, in the out of plane, are compatible with a pre-equilibrium mechanism of emission strongly related to the entrance channel.

In some of the spectra of ring G (fig. 5) is also quite evident an excess of particles of intermediate energy. A similar excess is also found in the spectra of ring C (not shown) but not in rings D and E (figs. 3 and 4), and is partially visible at some angles in the in-plane spectra (fig. 2). The angular and energy dependence of such a component is consistent with the well-established pattern for the near-scission emission: enhanced emission at angles perpendicular to the scission axis [27] with energies characteristic of emission barriers lower than those measured in the CE component. This correlation with scission axis, which is a sort of focusing effect, is remarkably evident when we compare the spectrum of ring D (fig. 3) at $\alpha = 105.5°$ and $\beta = 39°$ with the spectrum in the ring G (fig. 5) at $\alpha = 9.2°$ and $\beta = 42°$. The first detection position favours the detection of particles emitted out of plane along the direction of the scission axis; the second one favours the detection of particles emitted perpendicularly to the scission axis. In spite of the almost equal out-of-plane angles, we notice a dramatic difference in the intermediate-energy component.

From the fit to experimental spectra, alpha-particle multiplicities of 0.040 ± 0.006 and 0.014 ± 0.002, for pre-scission and post-scission emissions, respectively, have been deduced.

3.3 Evaporation residue channel

Evaporation residues were detected by four PPAC modules of the type described in sect. 2. In figs. 8 and 9 we show, as solid points, the number of protons and alpha-particles, respectively, detected in coincidence with one of the PPAC *versus* the identification number of the BALL detectors. Superimposed to the data is the result of the simulation performed with the code PACE2 (solid lines), in which the detailed geometry of the detecting system has been properly included. For each ring, we observe a strong dependence of the intensity on the detector position resulting from the different correlation angles with respect to the trigger detector, both for protons and alpha-particles. The same pattern of figs. 8 and 9 is observed for the case of the other trigger positions. The code PACE2 reproduces very well the observed pattern, independently of the ratio a_f/a_ν parameter, where a_f and a_ν are the level density parameters governing fission and particle evaporation, respectively. In the statistical model, this ratio is an input parameter which affects the competition between fusion-fission and fusion-evaporation, and hence, it is expected

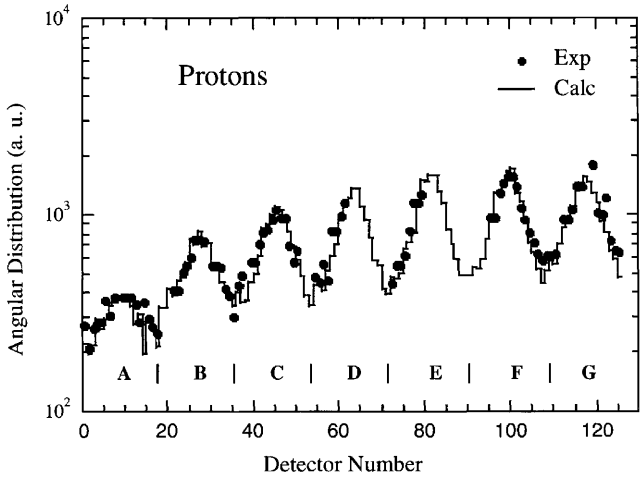

Fig. 8. Intensity distribution of protons in coincidence with the evaporation residues as a function of the BALL detectors grouped by rings.

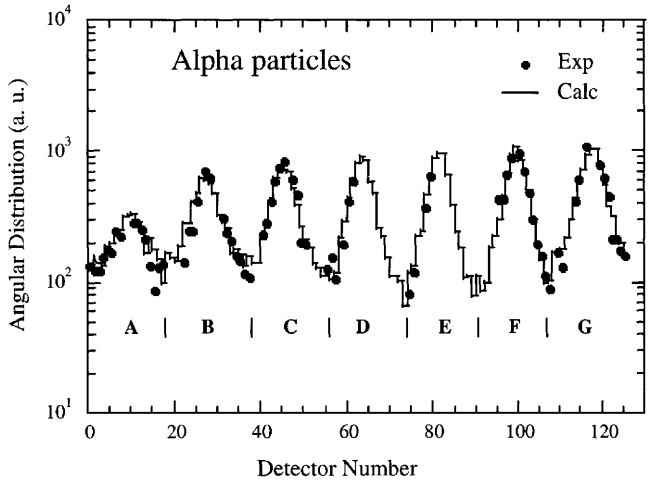

Fig. 9. Intensity distribution of alpha-particles in coincidence with the evaporation residues as a function of the BALL detectors grouped by rings.

Table 1. Calculated alpha-particle pre-scission multiplicities for different values of the a_f/a_ν parameter and delay time for the $^{32}S + ^{100}Mo$ system.

τ_d (10^{-21} s)	a_f/a_ν 1.00	a_f/a_ν 1.02	a_f/a_ν 1.04	a_f/a_ν 1.06	a_f/a_ν 1.08	a_f/a_ν 1.10
0	0.049	0.035	0.026	0.019	0.015	0.010
2	0.049	0.043	0.035	0.030	0.030	0.031
4	0.088	0.090	0.096	0.100	0.100	0.110

to have also an influence on the particle multiplicities in the ER channel.

Concerning the ER channel, we have extracted an estimate of the proton to alpha-particle multiplicity ratio, with the help of statistical model calculations. This also allowed us to optimize the ratio a_f/a_ν needed to analyse the pre-scission multiplicity. Since the calculations reproduce very well the shape of the angular distributions in figs. 8 and 9, independently upon the ratio a_f/a_ν, an estimate of the multiplicity ratio can be obtained by the code PACE2, provided that the model is also able to reproduce the measured angular distribution of the two particles, with a unique normalizing factor. Such a condition strongly depends upon the ratio a_f/a_ν and is not far from being fulfilled using the value $a_f/a_\nu = 1.08$ which provides the same normalizing factor within 30%, leading to a multiplicity ratio equal to 1.48. The implications of the use of such a value of a_f/a_ν in the model are discussed in the next section.

4 Results and conclusions

We have analyzed the pre-scission alpha-particle multiplicity M_α^{PRE} on the basis of the statistical model as implemented in the code PACE2. A fission time parameter τ_d has been included into the code so that the fission probability is zero up to the time τ_d and has full statistical value subsequently. Since we expect that the particle multiplicities are sensitive to the value of the ratio a_f/a_ν and to the delay time τ_d we performed a grid of calculations for $1.00 \leq a_f/a_\nu \leq 1.10$ and $0 \leq \tau_d \leq 4 \times 10^{-21}$ s. The results for M_α^{PRE} are given in table 1. The calculations show that the experimental value of 0.04 can be reproduced with $\tau_d = 0$ and $a_f/a_\nu = 1.0$. If we consider the result of the analysis in the evaporation residue channel, we should consider $a_f/a_\nu = 1.08$ and $\tau_d \approx 2 \times 10^{-21}$ s as our optimal delay time. A further increase in τ_d is not compatible with our data because it would produce a rapid increase of M_α^{PRE}. We also notice that such an increase in τ_d would completely wash out the dependence of M_α^{PRE} on a_f/a_ν shown for $\tau_d = 0$.

Therefore, on the basis of our simple static calculation, we can conclude that no significant dynamical effects have been evidenced in the alpha-particle pre-scission emission in the 240 MeV $^{32}S + ^{100}Mo$ system. From the systematics on the threshold excitation energy for the appearance of a non-statistical behavior of the fission process [15], we would have expected a sizable deviation from the statistical description in the pre-scission particle multiplicities. In fact, a reliable extrapolation of the data of ref. [15] to lower masses of the compound nucleus would give a value of 80 MeV as threshold energy for our system, to be compared to the excitation energy of 152 MeV in the present experiment.

Table 2. Calculated cross-sections in mb for the $^{32}S + ^{100}Mo$ system.

Lab energy (MeV)	160	170	200	240
Evaporation	994	1010	904	779
Fission	32	130	353	268
Fast fission			47	410

Results in agreement to our present findings have been reported in the system of similar fissility Ar + Ag [21] which was measured at two excitation energies, $E_x = 128$, 194 MeV [1]. Although these energies are well above the threshold expected on the basis of the predictions in ref. [15], short delay times have been found: $\tau_d = 4$ and 5×10^{-21} s for the two excitation energies, respectively [21]. On the other hand, for this system Britt *et al.* [30] obtained a critical angular momentum for fusion of $105\hbar$, larger than the value of the angular momentum for which the fission barrier vanishes, $l_{B_f} = 91\hbar$, obtained by the rotating-liquid-drop model. This finding supports the presence of the fast-fission process which would result in an overall lowering of the measured fission time. Fast fission is considered to be a mechanism intermediate between compound-nucleus formation and deep-inelastic reactions which occurs as soon as the angular momentum gets larger than l_{B_f} [31], even though there are recent indications that this process can take place even at angular momenta lower than l_{B_f} [32].

In order to investigate if our results could reflect the contribution from other mechanisms producing fragments similar to the fission fragments, but with faster time scale, we performed calculations of the cross-sections for the production of evaporation residues, for the fission and fast-fission processes, at different incident energies, using the code PACE2. We used the critical angular momentum for fusion deduced by the Bass model [33] and the value of l_{B_f} from the FRLD model [34]. Results are reported in table 2.

Although these values may only be taken as an indication, it appears that at 240 MeV fast fission may play a significant role. In fact, the calculated critical angular momentum for fusion is $90\hbar$ which is greater than the angular momentum at which the fission barrier vanishes ($83\hbar$). The overall picture at 200 MeV appears different, as fast fission cross-section is greatly reduced while fission and evaporation cross-sections increase. Moreover, deep inelastic at 200 MeV will be lower than at 240 MeV and also contamination, if present, will be lower. On these grounds, a measure at 200 MeV can be very useful to understand the reaction mechanisms involved.

We thank the accelerator crew of the Laboratori Nazionali di Legnaro for providing excellent beams. Technical support from M. Caldogno during the experiment is gratefully acknowledged.

References

1. R. Lacey, N.N. Ajitanand, J.M. Alexander, D.M. de Castro Rizzo, G.F. Peaslee, L.C. Vaz, M. Kaplan, M. Kildir, G. La Rana, D.J. Moses, W.E. Parker, D. Logan, M.S. Zisman, P. DeYoung, L. Kowalski, Phys. Rev. C **37**, 2540 (1988).
2. D.J. Hinde, D. Hilscher, H. Rossner, B. Gebauer, M. Lehmann, M. Wilper, Phys. Rev. C **45**, 1229 (1992).
3. H. Ikezoe, Y. Nagame, I. Nishinaka, Y. Sugiyama, Y. Tomita, K. Ideno, S. Hamada, N. Shikazono, A. Iwamoto, Phys. Rev. C **49**, 968 (1994).
4. J.P. Lestone, J.R. Leigh, J.O. Newton, D.J. Hinde, J.X. Wei, J.X. Chen, S. Elfstrom, M. Zielinska-Pfabé, Nucl. Phys. A **559**, 277 (1993).
5. A. Saxena, A. Chatterjee, R. Choudhury, S.S. Kapoor, D.M. Nadkarni, Phys. Rev. C **49**, 932 (1994).
6. W.E. Parker, M. Kaplan, D.J. Moses, J.M. Alexander, J.T. Boger, R.A. Lacey, D.M. de Castro Rizzo, Nucl. Phys. A **568**, 633 (1994).
7. A. Chatterjee, A. Navin, S. Kailas, P. Singh, D.C. Biswas, A. Karnik, S.S. Kapoor, Phys. Rev. C **52**, 3167 (1995).
8. L. Fiore, G. D'Erasmo, D. Di Santo, L. Celano, N. Colonna, E.M. Fiore, A. Pantaleo, V. Paticchio, G. Tagliente, G. Viesti, D. Fabris, G. Nebbia, M. Cinausero, E. Fioretto, G. Prete, A. Brondi, G. La Rana, R. Moro, E. Vardaci, F. Lucarelli, P.F. Bortignon, Nucl. Phys. A **620**, 71 (1997).
9. R. Butsch, D.J. Hofman, C.P. Montoya, P. Paul, Phys. Rev. C **44**, 1515 (1991).
10. D.J. Hofman, B.B. Back, P. Paul, Phys. Rev. C **51**, 2597 (1995).
11. V.A. Rubchenya, A.V. Kuznetsov, W.H. Trzaska, D.N. Vakhtin, A.A. Alexandrov, I.D. Alkhazov, J. Äystö, S.V. Khlebnikov, V.G. Lyapin, O.I. Osetrov, Yu.E. Penionzhkevich, Yu.V. Pyatkov, G.P. Tiourin, Phys. Rev. C **58**, 1587 (1998).
12. I. Diószegi, N.P. Shaw, I. Mazumdar, A. Hatzikoutelis, P. Paul, Phys. Rev. C **61**, 024613 (2000).
13. N.P. Shaw, I. Diószegi, I. Mazumdar, A. Buda, C.R. Morton, J. Velkovska, J.R. Beene, D.W. Stracener, R.L. Varner, M. Thoennessen, P. Paul, Phys. Rev. C **61**, 044612 (2000).
14. E. Vardaci, G. La Rana, A. Brondi, M.A. Di Meo, R. Moro, A. Principe, D. Fabris, G. Nebbia, G. Viesti, G. Prete, *International Conference on Dynamical Aspects of Nuclear Fission*, edited by Yu.Ts. Oganessian, J. Kliman, S. Gmuca (World Scientific, Singapore, 2000).
15. M. Thoennessen, G.F. Bertsch, Phys. Rev. Lett. **71**, 4303 (1993).
16. A. Kramer, Physica (Amsterdam) **7**, 284 (1940).
17. V.A. Rubchenya, *Proceedings of the International Conference Large-Scale Collective Motion of Atomic Nuclei, October 15-19,1996, Brolo, Messina, Italy*, edited by G. Giardina, G. Fazio, M. Lattuada (World Scientific, Singapore, 1997) p. 534.
18. G. Giardina, *Proceedings of the VI International School-Seminar on Heavy Ion Physics, September 22-27, 1997, Dubna, Russia*, edited by Yu.Ts. Oganessian, R. Kalpakchieva (World Scientific, Singapore, 1998) p. 628.
19. A.K. Dhara, K. Krishan, C. Bhattacharya, S. Bhattacharya, Phys. Rev. C **57**, 2453 (1998) and references therein.
20. M.G. Itkis, A.Ya. Rusanov, Phys. Part. Nucl. **29**, 160 (1998).
21. G. La Rana, E. Vardaci, A. Brondi, M.A. Di Meo, R. Moro, C. Basile, D. Fabris, G. Nebbia, G. Viesti, M.Cinausero, E. Fioretto, G. Prete, F. Lucarelli, N. Gelli, *Proceedings of the International Conference on Nuclear Reaction Mechanisms, June 5-9, 2000, Varenna, Italy*, edited by E. Gadioli (Ricerca Scientifica ed Educazione Permanente, Grafiche Vadacca, Vignate (MI), 2000).
22. E. Fioretto, M. Cinausero, M. Giacchini, M. Lollo, G. Prete, R. Burch, M. Caldogno, D. Fabris, M. Lunardon, G. Nebbia, G. Viesti, A. Boiano, A. Brondi, G. La Rana, R. Moro, A. Ordine, E. Vardaci, A. Zaghi, N. Gelli, F. Lucarelli, IEEE Trans. Nucl. Sci. **44**, 1017 (1997).
23. A. Ordine, A. Boiano, E. Vardaci, A. Zaghi, A. Brondi, IEEE Trans. Nucl. Sci. **45**, 873 (1998).
24. E. Vardaci, *VISM: a Computer Program for Nuclear Data Analysis*, Annual Report Carnegie Mellon University, Pittsburgh, USA (1989).
25. N.N. Ajitanand, R. Lacey, G.F. Peaslee, E. Duek, J.M. Alexander, Nucl. Instrum. Meth. Phys. Res. A **243**, 111 (1986).
26. N.N. Ajitanand, G. La Rana, R. Lacey, D.J. Moses, L.C. Vaz, G.F. Peaslee, D.M. de Castro Rizzo, M. Kaplan, J.M. Alexander, Phys. Rev. C **34**, 877 (1986).
27. E. Duek, N.N. Ajitanand, J.M. Alexander, D. Logan, M. Kildir, L. Kowalski, L.C. Vaz, D. Guerreau, M.S. Zisman, M. Kaplan, Phys. Lett. B **131**, 297 (1983).
28. L. Schad, H. Ho, G.-Y. Fan, D. Lindl, A. Pfoh, R. Wolski, J.P. Wurm, Z. Phys. A **318**, 179 (1984).
29. E. Vardaci, M. Kaplan, W.E. Parker, D.J. Moses, J.T. Boger, G.J. Gilfoyle, M.A. McMahan, M.Montoya, Phys. Lett. B **480**, 239 (2000).
30. H.C. Britt, B.H. Erkkila, R.H. Stokes, H.H. Gutbrod, F. Plasil, R.L. Ferguson, M. Blann, Phys. Rev. C **13**, 1483 (1976).
31. C. Ngô, C. Grégoire, B. Remaud, E. Tomasi, Nucl. Phys. A **400**, 259c (1983).
32. D.H. Hinde, A.C. Berriman, M. Dasgupta, J.R. Leigh, J.C. Mein, C.R. Morton, J.O. Newton, Phys. Rev. C **60**, 054602 (1999).
33. R. Bass, *Nuclear Reactions with Heavy Ions*, (Springer-Verlag, New York, 1980).
34. A.J. Sierk, Phys. Rev. C **33**, 2029 (1986).